

# TRAVELLING WAVE FAULT LOCATION for RADIAL MV DISTRIBUTION SYSTEMS, THEORITICAL APPROACH and EMTP SIMULATIONS

A. Valenti\*, G. Huard\*, P. Johannet\*, F. Brouaye\*\*, P. Bastard\*\*\*

(\*) Electricité De France

Direction des Etudes et  
Recherches.

Clamart, France.

e-mail : arnaud.valenti@edf.fr

(\*\*) SUPELEC-CNRS

Département de Recherche en  
Electromagnétisme.

Gif sur Yvette, France.

e-mail : brouaye@supelec.fr

(\*\*\*) SUPELEC

Service Electrotechnique et  
Electronique Industrielle.

Gif sur Yvette, France.

patrick.bastard@supelec.fr

**Abstract :** This paper deals with remote location of a single ground fault in a Medium Voltage distribution system. The study is based on the travelling wave method and the principle is to study the reflections which occur in a MV radial distribution system (since there is a sudden impedance change especially at the location of the fault). Theoretically, these reflections create characteristic frequencies in currents and voltages. Indeed, the solution of the initial 3-dimensional differential equation (telegraphs equation for 3-phase system) determines resonant frequencies depending on the reflection coefficients.

Many EMTP (ElectroMagnetic Transient Program) simulations confirm this theory which can be applied to cables and overhead lines. Some simple grid topologies have been tested : single cables, single overhead lines, cable + overhead line, cable + overhead line with two branches.

Some field tests have also been performed and several signal processing methods have been tested to extract the frequency information related to the fault distance from the signal (current and voltage).

**Keywords:** MV Distribution networks, fault location, travelling wave, reflection, EMTP simulations, single phase faults.

## I. INTRODUCTION

### A. Faults on MV distribution system

From 1990, as part of the examination of MV systems, EDF broached the issue of locating steady state and also transients faults causing a large number of short failures in these systems. This location would increase the efficiency of actions to restore networks to their appropriate level and also to guide investment and maintenance decisions, in order to improve the quality of the energy delivered by MV systems, as well as to extend the life-time of these facilities. It may be envisaged either to forestall the occurrence of possible faults or to eliminate them without customers noticing any disturbance. For that, since a self extinguished fault is detected in the substation, it would be convenient to locate it and to fix it before it gets worse.

Since there are numerous kinds of faults encountered in MV networks (duration, number of phases involved), the study has been restricted to the single phase to ground fault which are the most frequent. The neutral point connection considered is compensated, regarding the future evolution of the French distribution system.

### B. Fault location with impedance calculation

A study about fault location using low frequency impedance calculations ([1]), has been carried out in the LEG Grenoble in collaboration with EDF.

The approach is based on the frequency analysis of the current oscillation during the charge of the two unfaulted phases after the occurrence of a single phase to earth fault. This frequency charge around 200 Hz depends on the fault distance, the fault resistance and the capacitance of the whole system so the method is the following one :

- signal processing for evaluation of the right frequency
- modeling of the radial distribution system
- fault resistance estimation
- numerical resolution and determination of the fault position

The fault resistance has been identified as the most important parameter acting on the results, and the influences of the conductor parameters, the load, or the system's structure are not significant. Moreover the fault position determines the charge frequency (the more distant the fault , the lower the charge) and the FFT observation window has to be chosen consequently. The accuracy of this method can be improved through a suitable signal processing.

### C. Fault location with travelling wave method

A totally different approach is described in this paper. The travelling wave method is actually used for HV distribution system ([2]) : the time interval between two pulses corresponding to reflections in the line (end or fault) is measured (using different methods like in [3-6]) and the distance to the fault is calculated using the velocity of the propagation. But, for MV distribution systems, the problem becomes more complex because the topology in radial grid involves many reflections.

## II. THEORY

### A. Presentation of the problem

Consider a 3-phase overhead line with impedance  $Z_0$  and  $Z_{def}$  ( $3 \times 3$  matrices) at the two ends.

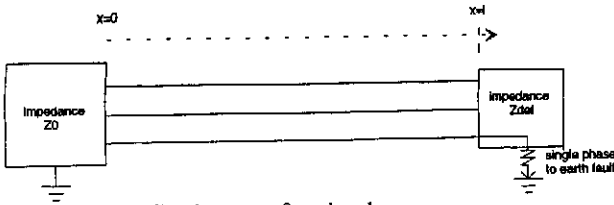


Figure II-1 : reflection at  $x=0$  and  $x=l$

## B. Solution of the telegraphs equation

### 1) Initial equations

$Z$  and  $Y$  are the line impedance and admittance matrices of the line, respectively.

$$\frac{d^2 V(x)}{dx^2} = ZY V(x) \quad (1)$$

and 
$$\frac{d^2 I(x)}{dx^2} = YZ I(x). \quad (2)$$

### 2) Modal analysis ([7-8-9])

$$D_v = M^{-1} Z Y M \quad (4)$$

where  $D_v$  is diagonal and  $M$  is the eigenvector base.

$$D_i = N^{-1} Y Z N \quad (5)$$

where  $D_i$  is diagonal and  $N$  is the eigenvector base.

$D_v = D_i$ , see [5] and  $\Gamma$  is defined such that :

$$D_i = \Gamma^2 \quad (6)$$

appearance of three independent modes : ground mode, and two aerial modes.

### 3) General solutions

(the base is provided by the eigenvectors) :

$$V_m(x) = e^{\Gamma x} V_{mi} + e^{-\Gamma x} V_{mr} \quad (7)$$

$$I_m(x) = e^{\Gamma x} I_{mi} + e^{-\Gamma x} I_{mr} \quad (8)$$

### 4) Characteristic impedance and admittance

It is useful to define for the line :

■ the characteristic impedance  $Z_c = \Gamma^{-1} N^T Z N$  (9)

■ the characteristic admittance  $Y_c = \Gamma^{-1} M^T Y M$  (10)

### 5) Boundary conditions

The terms  $V_{mi}$ ,  $V_{mr}$  will be determined by the boundary conditions. Let us consider the beginning base defined by the three phases in which  $J(p)$  is the current source provoked by the fault, these terms are written :

$$\begin{cases} I(l, p) = J(p) - Y_{def} V(l, p) \\ I(0, p) = Y_0 V(0, p) \end{cases} \quad (11)$$

which gives the system :

$$\begin{cases} (Y_{def} + Z^{-1}\Gamma)e^{\Gamma l} M V_{mi} + (Y_{def} - Z^{-1}\Gamma)e^{-\Gamma l} M V_{mr} = J(p) \\ (Y_0 - Z^{-1}\Gamma) M V_{mi} + (Y_0 + Z^{-1}\Gamma) M V_{mr} = 0 \end{cases} \quad (12)$$

(Same for current, see [8]).

Note that  $Z^{-1}\Gamma$  corresponds to the inverse of a characteristic impedance, except for base change coefficients.

### 6) Reflection coefficients

Let us now denote the reflection coefficient of a system with three conductors at  $x = 0$ , as  $Kr_0$  (by definition

$$M V_{mr} = Kr_0 \cdot M V_{mi} ) :$$

$$Kr_0 = -(Y_0 + Z^{-1}\Gamma)^{-1} (Y_0 - Z^{-1}\Gamma). \quad (13)$$

Similarly, let us denote the coefficient of reflection at  $x = l$ , at the location of the fault, as  $Kr_{def}$  :

$$Kr_{def} = -(Y_{def} + Z^{-1}\Gamma)^{-1} (Y_{def} - Z^{-1}\Gamma) \quad (14)$$

### 7) General solution of the differential equation, except for a multiplication factor, for $0 \leq x \leq l$

Solution of system (12) :

$$\begin{aligned} V(x, p) &= A(x) \left( e^{\Gamma l} - Kr_{def} Kr_0 e^{-\Gamma l} \right)^{-1} B J(p) \\ \text{where } A(x) &= \left( e^{\Gamma x} + Kr_0 e^{-\Gamma x} \right) \\ \text{and } B &= (Y_{def} + Z^{-1}\Gamma)^{-1} \end{aligned} \quad (15)$$

## C. Theoretical results

The previous expression may be processed with MATLAB, and  $V(0, f)$  and  $I(0, f)$  are thus calculated as a function of the frequency  $f$ .

Several configurations (cables, overhead lines, transformers, short circuit, etc.) have been tested and the influence of some parameters such as the fault resistance and obviously the lengths involved, have been investigated. This study shows that :

- For each mode, the significant resonant frequencies are directly related to the following expression :

$$\left( e^{\Gamma l_0} - Kr_{def} Kr_0 e^{-\Gamma l_0} \right)^{-1}.$$

- The ground mode seems to be less present since it is more damped. (With this kind of calculation, the three modes are clearly separated).
- If reflection coefficients are independent of the frequency in the studied range, then the two poles that are likely to occur are  $e^{-2\gamma l}$  (peaks at frequencies  $f = k \frac{c}{2l}$ ,  $k$  integer  $> 0$ ) and  $-e^{-2\gamma l}$  (peaks at

frequencies  $f = (2k + 1) \frac{c}{4l}$ ,  $k \geq 0$ ); this depends on

the behavior of  $Kr_{def}$  and  $Kr_0$ . Consequently, it is important not to forget that impedance values at each end of the segment which includes a fault, determine reflection coefficients and therefore the resonant frequencies characteristic of the length of the segment and the location of the fault.

- As predicted, peaks are directly related to the lengths involved.
- However in most cases (nodes or line cable junctions), the reflection coefficients depend, more or less, on the frequency and consequently resonant frequencies are slightly offset from the above values which makes the problem considerably more complex.

- The fault resistance has almost no influence on position of the peak that reveals the location of the fault, but it does determine its amplitude and therefore the possibility of detecting it.
- Similarly, conductor parameters (conductivity, diameter, position in space) have very little influence on the results. The propagation speed varies little as a function of these high frequency parameters.

#### D. Conclusion

In a 3-phase system, propagation phenomena are characterized essentially by two propagation modes, namely ground mode and aerial mode.

In particular, they demonstrate the location of a single phase earth fault in a overhead line segment, through significant frequencies related to propagation velocity. These frequencies are not very dependent on the resistance of the fault, or on the line parameters. However, due to reflections, they are dependent on the impedance downstream and upstream from the segment in fault as shown in a previous work [8]. This means that these frequencies are not related simply to the lengths involved as it is the case if the reflections are of the short circuit or open-ended line type. It is also necessary to know if these results which are valid for the faulted segment are the same if the measurements are made at the source substation. In other words, will all these frequencies reach the substation without being modified along the path that separates the segment in fault from the substation. This will be checked with the help of EMTP simulations.

### III. EMTP SIMULATIONS

Simple cases are presented in the following section.

#### A. Influence of line parameters and the fault resistance :

This kind of work has already been done in [9] for EHV (400kV) transmission lines.

##### 1) system modeling

The objective is to inject a voltage of 1V into one phase of a 900m three-phase 20kV line and to monitor the influence of line parameters.

The reference system is shown in figure III-1, in which R=10 Ohm and the line parameters (see [10]) are as follows :

- conductor resistance : 0.22 Ohm/km.
- conductor diameter : 1.5 cm
- average height of the 3 conductors above the ground : 8.2 m. (Value computed by EMTP).
- horizontal distance between two adjacent conductors : 1.5 m
- excitation type : single phase
- resistivity of the ground : 100 Ohm.m
- line model : frequency dependent (FD-LINE)

=> Under these conditions, the dominant frequency measured at open end by the simulation is then  $f_0 = 78800\text{Hz}$ .

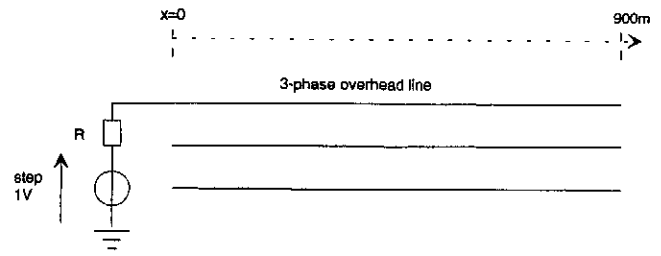


Figure III-1 : 3-phase overhead line, length=900 m.

##### 2) results

EMTP simulations on this simple case were used to study the influence of line parameters and the fault resistance on the required frequencies. The results are given in table III-1 below.

Table III-1 : Characteristic frequency of the length of the line.

parameter	value	frequency (Hz)	$\Delta f / f_0$ (%)
R (Ohm)	10	78800	0
	1	78800	0
height (m)	11.2	80200	1.8
	5.8	77400	1.8
horizontal distance (m)	2.5	78800	0
	1	78800	0
diameter (cm)	0.5	79300	0.6
	2.5	78400	0.5
resistance (Ohm/km)	0.32	78800	0
	0.12	78800	0
resistivity of the ground (Ohm.m)	200	77500	1.6
	50	79600	1.0
excitation	ground mode	75300	4.4
	aerial mode	83100	4.2
two unfaulted phases in short circuit to earth at x=0		83100	aerial mode

##### 3) conclusion :

- The unbalanced line to ground fault involves a modal mixing.
- The fault resistance affects the power of the resonant frequency that produces the fault, but not its value. Finally, if this fault resistance is low enough so that the corresponding resonant frequency is accessible, then this frequency will be independent of the value of the resistance.
- The height at which the conductor is located and the resistivity of the ground are the only parameters that slightly change the propagation speed and therefore the required frequency. (For the influence of the resistivity of the ground, see [9]). Otherwise, the characteristic parameters of conductors have practically no influence on the results, in other words the values of the required frequencies. Hence, the method is robust to variations in system parameters.
- If the two unfaulted phases are short circuited to earth at one end, then the aerial mode is preponderant.

B. fault on a 3-phase overhead line :

1) System modeling :

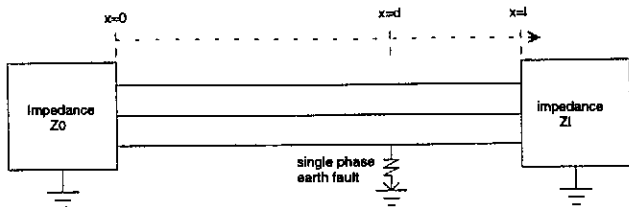


Figure III-2 : line alone (theoretical case), fault at distance  $x=d$ .

•  $Z_0 = Z_t // Z_f$  where  $Z_t$  represents the transformer + the cables in the substation and  $Z_f$  represents the other outgoing feeders (capacitance C) + the connection impedance (inductance L). The capacitance C is actually used for generating a short-circuit type reflection at the substation and moreover these capacitances are used in the experiment field (for other studies at low frequency). For high frequencies  $Z_t // Z_f$  is equivalent to  $Z_f$ .

$$Z_0 \approx Z_f = \begin{pmatrix} Lp + \frac{1}{Cp} & 0 & 0 \\ 0 & Lp + \frac{1}{Cp} & 0 \\ 0 & 0 & Lp + \frac{1}{Cp} \end{pmatrix}$$

where  $\begin{cases} L = 10^{-2} \text{ mH} \\ C = 30 \mu\text{F} \end{cases}$  and where p is the Laplace variable.

This gives an impedance of 1.33 Ohm at 100 kHz. (Which is low compared with the characteristic impedance of the line, hence a short circuit type reflection).

•  $Zl = \infty$ , open-ended line.

2) graph for  $L=0.01 \text{ mH}$

A step of 20000 V (tripping of a load switch) is simulated at the fault (resistance 20 Ohms) located at  $d = 220 \text{ m}$  in a line with length  $l = 630 \text{ m}$ .

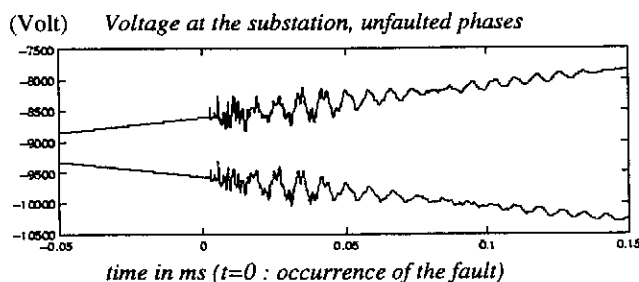
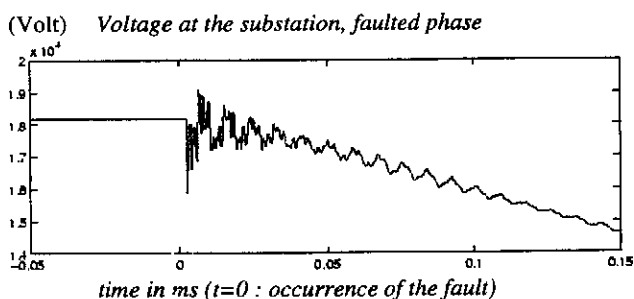


Figure III-3 : Voltages vs. time.

The following figure III-4 shows a FFT of two voltages measured at  $x=0$ , one on the faulted phase (solid) and the other on the unfaulted phase (dotted).

These values have been chosen because they match the scale of the experimental network built by EDF which will be described hereafter.

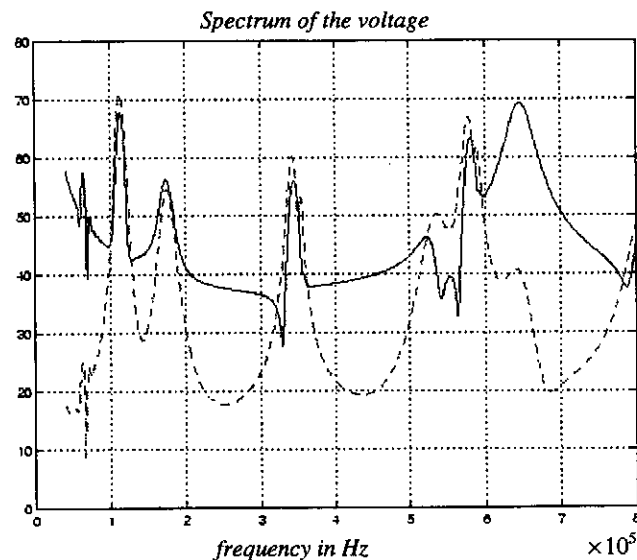


Figure III-4 : Comparison between faulted phase (solid) and unfaulted phase (dotted).

The first peak at 114 kHz represents the length of the overhead line  $l=630 \text{ m}$ . Considering aerial mode :

$$f = \frac{299000}{4 * 0.63} = 119 \text{ kHz}.$$

The second peak at 175 kHz represents the length of the downstream line  $l=410 \text{ m}$ . Considering aerial mode :

$$f = \frac{299000}{4 * 0.41} = 182 \text{ kHz}.$$

The third peak at 345 kHz is  $3 * 114 \text{ kHz}$  etc.

And the fault appears on the faulted phase (solid) at 645 kHz. Considering direct mode :

$$f = \frac{299000}{2 * 0.22} = 680 \text{ kHz}.$$

Therefore, there is a difference of about 5% between the predicted values for aerial mode if perfect short circuit or open-ended line reflections are considered. But if the impedance  $Z_0$  drops (smaller L), the value becomes closer and closer to 680 kHz.

For instance, if  $L=0.001 \text{ mH}$ , the fault appears at 663 kHz, which proves clearly that the resonant frequencies are actually dependent of the impedance at the end of the faulted segment.

3) conclusion

The characteristics of the substation (transformer + various junctions) and other feeders modify the observed frequencies from the values given by the simple relations in section II-C. The impedance of the assembly (source substation + unfaulted outgoing feeders) offsets the frequency peaks, for example as shown by the variations of L. Therefore in the future, this offset concept should be

defined quantitatively in order to be able to relate the frequency to the length involved.

C. Case : cable + overhead line

1) system modeling

This case represents one of the miscellaneous configuration of the experimental grid built by EDF whose tests will be presented in section IV.

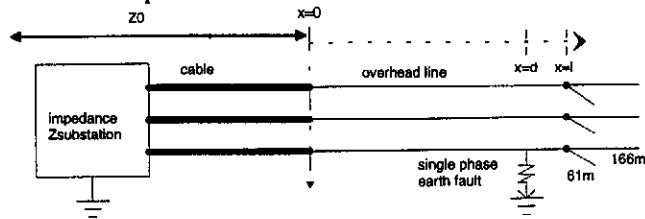


Figure III-5 : scheme of the system

For this study the basic values are the following : length of the cable : 320 m ;  $d = 585$  m ;  $l = 630$  m, at this point there is a node and the line continues with two branches of respectively 61 m and 166 m (open-ended line at the end).

$Z_{substation}$  is equivalent to the same impedance  $Z_f$  as in section III-B-1.  $L = 10^{-2}$  mH and  $C = 30$  nF .

2) Spectrum

The figure III-6 below represents the spectrum of the voltage at the substation.

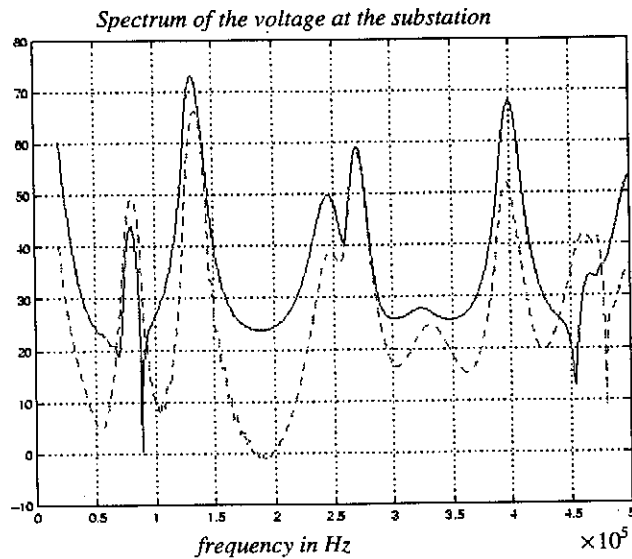


Figure III-6 : faulted phase (solid) unfaulted phase (dotted).

The fault appears at 245 kHz ( $f=c/4l$  gives 255 kHz) and the length of the whole overheadline segment in fault appears at 85 kHz ( $f=c/4l$  gives 94 kHz, with  $l=630+166=796$  m).

The length of the cable appears at 135 kHz ( $f=c/4l$  gives 139 kHz).

3) Conclusion

As before, the value of  $L$  in  $Z_f$  , if it increases, offsets the resonant frequency of the cable towards the left. The distinctive frequency of the fault is present but the cable frequency is the most powerful frequency.

Remark : if an inductance is added between the cable and the line in order to represent the junction, then the peaks for the fault and the overhead line are also offset towards the left. This will help us later to explain the experimental results.

IV. FIRST REAL EXPERIMENTS

A. The short scale distribution system

A Medium Voltage distribution grid was built by EDF in 1995 following usual network construction techniques. It has been used to produce and duplicate two main types of anomalies (direct contacts with ground, and flashover insulators), at different places.

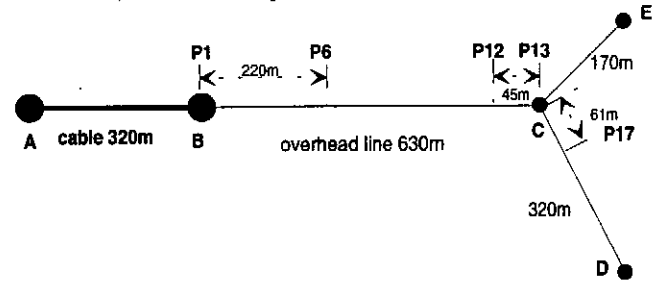


Figure IV-1 Experimental network

In the following, the tests considered correspond to a configuration with a fault at P12 (tower number 12), open-ended circuit at P17 (tower number 17 ; note that it was not technically possible to disconnect the whole branch CD). The measurements are carried out at the substation.

B. Signal processing

Let us just mention that the experimental data acquired at 1 MHz were initially analyzed by a Short Time Fast Fourier Transform (in the time-frequency domain). The observation window in which the fault is the most clearly marked is then selected for a spectral analysis using a Fast Fourier Transform (Welch method).

Note that the results given by standard methods for estimating the spectrum (applied to a larger window) may not be good. The searched frequencies are less well defined since the signature of the fault at high frequency is damped very quickly and therefore the observation window must be positioned as precisely as possible in time when the fault appears.

C. Experimental results

The configuration of the experimental tests is the same as described in the EMTP simulations chapter III-C-1 : open-ended line in P17 and fault in P12.

For each test the voltage and the current are measured at the substation and then the frequency spectrum of the three phases of a test (for current and voltage) is computed with MATLAB routines. Figure IV-2 (time domain) and Figure IV-3 (frequency domain) shows the exemple of one of these tests.

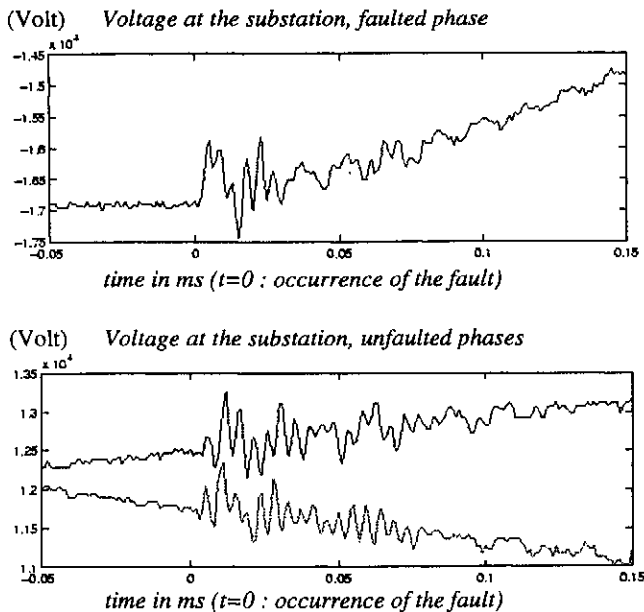


Figure IV-2 : Voltage vs. time for the three phases.

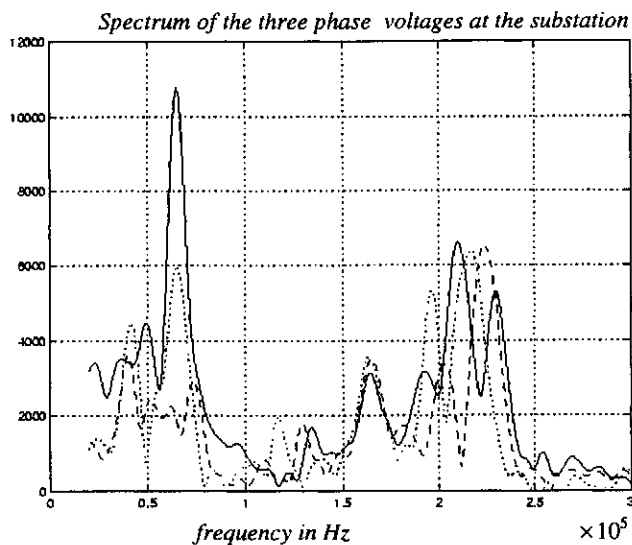


Figure IV-3 : FFT of the voltage of the 3 phases measured in the substation. Faulted phase in solid line, unfaulted phases in dashed and dotted lines.

As predicted by theory, it would appear that the location of the fault is demonstrated by one of the dominant frequencies between 190 and 230 kHz, certainly the most powerful around 210 kHz (faulted phase in solid). This test shows that there should be high frequencies related to distance in the grid, however it is still too early to see exactly what corresponds to each frequency on each phase.

## V. CONCLUSION

This article demonstrates that propagation phenomena in MV lines and cables initiate characteristic frequencies that are likely to be related to the lengths of conductors between two impedance changes. This may be applied to fault localizing, since the appearance of a single phase earth fault may be considered as being the injection of a voltage surge at the location of the fault which will create a wave propagating throughout the network and be reflected at each impedance change. Spectral analyses carried out on EMTF simulations effectively demonstrate frequencies that correspond to various reflections of the wave created by the fault, and which therefore provide information that can be used to determine its location.

However, the relation between this frequency and the distance to which it corresponds depends on impedance at the ends involved which makes localization inaccurate. (Problem of peaks being offset from the simple case of the half-wave case  $c/2l$  or the quarter-wave case  $c/4l$ ). Furthermore, experimental results that confirm high frequency phenomena, probably contain information related to the fault distance, but what they show most clearly is that there is still a lot of work to be done in high frequency modeling of a MV network. There are still a lot of uncertainties in the high frequency behavior of the transformer (differences between the three phases), and on the role played by all junctions.

## VI. REFERENCES

- [1] T. Wellfonder, *Localisation de défauts monophasés dans les réseaux de distribution à neutre compensé*, PHD work in the LEG Grenoble, 1998.
- [2] P.A. Crossley, P.G. Mc Laren, « Distance protection based on travelling waves », *IEEE Transactions on Power Apparatus and Systems*, Vol. PAS-102, No. 9, September 1983.
- [3] E.H. Shehab-Eldin, P.G. Mc Laren, « Travelling wave distance protection. Problem areas and solutions ». *IEEE Transactions on Power Delivery*, Vol. 3, No. 3, July 1988.
- [4] C. Christopoulos, D.W.P. Thomas, A. Wright, « Signal processing and discriminating techniques incorporated in a protective scheme based on travelling waves », *IEE Proceedings*, Vol. 136, No. 5, September 1989.
- [5] G.B. Ancell, N.C. Pahalawaththa, « Maximum likelihood estimation of fault location on transmission lines using travelling waves ». *IEEE Transactions on Power Delivery*, Vol. 9, No. 2, April 1994.
- [6] F.H. Magnago, A. Abur, « Fault location using wavelets », *IEEE Transactions on Power Delivery*, Vol. 13, No. 4, October 1998.
- [7] P. Johannet, *Constantes linéiques des lignes et des câbles : formulaire pour le calcul des chutes de tension et des phénomènes de propagation*, note EDF-DER Clamart, Juillet 1998.
- [8] A. Valenti, *Localisation à distance des défauts sur les réseaux HTA, méthode de propagation et réflexion des ondes, approche théorique*, note EDF-DER Clamart, Juillet 1998.
- [9] G.B. Ancell, N.C. Pahalawaththa, « Effects of frequency dependence and line parameters on single ended travelling wave based fault location scheme », *IEE Proceedings-C*, Vol. 139, No.4, July 1992, pp 332-342.
- [10] « EMTF, Version 3.0, Rule Book 2, Auxiliary Routines », Section 10, Line Constants Routines, November 1996.